How pantograph electric arcs affect energy efficiency in DC railway vehicles

How Pantograph Electric Arcs affect Energy Efficiency in DC Railway Vehicles

Andrea Mariscotti
DITEN, University of Genova, Genova, Italy
andrea.mariscotti@unige.it

Domenico Giordano
INRIM, Torino, Italy
d.giordano@inrim.it

Antonio Delle Femine, Daniele Gallo
University of Campania "L. Vanvitelli", Aversa, Italy
antonio.dellefemine@unicampania.it
daniele.gallo@unicampania.it

Davide Signorino
INRIM, Politecnico di Torino, Italy
d.signorino@inrim.it

***Abstract*—In DC electrified railways pantograph electric arcs represent not only a disturbance, but the step change of the pantograph voltage affects power losses directly and indirectly. The available line voltage is reduced if the train is in traction condition, the arc itself is characterized by ohmic power losses, and the triggered oscillating transient responses are characterized by a net power loss. In addition, if arc occurs during braking the arc voltage suddenly increases the pantograph voltage and may interfere with the dissipative braking chopper, reducing the recovered energy. This work presents the model and analysis of these phenomena with experimental results for arcs measured on a 3 kV dc line in traction and braking conditions.**

***Keywords*—Electric arc, Energy consumption, Power Quality, Power supply transient, Power system transients, Rail transportation, Rolling Stock**

I. Introduction

Electric arcs are still nowadays an unavoidable by-product of the current collection by sliding contact in electrified transportation systems and are particularly intense for dc traction supplies. The power level is significant: up to several MW per sliding contact in railways with overhead contact line (OCL), lower in metros with third rail distribution that share at least one sliding shoe per coach. The power transfer from the OCL to the carbon blade of the pantograph during train movement occurs through a contact section of a few square millimetres. As soon as the current collection mechanism worsens due to imperfection of the geometry, defects on surfaces, temporary detachment, debris, oxidation, arcing occurs with air ionization and plasma conduction. The temperature increases to the melting point of materials and only train movement and air convection avoid the degeneration into an extended irreversible damage of surfaces or complete OCL breakage.

Arc intensity and duration depends on several parameters characterizing the train: its speed, the intensity of the dc current, the traction or braking condition. Although dc arcs are more intense than those in ac railways, the latter have recently received much more attention, as pointed out in [1][2]. DC railways in general (so encompassing all the metro, light railways, tramways, etc. using a dc supply) undergo more intense arcing due to two factors: the supply is a dc voltage of significant amplitude (between 600 V and 3000 Vdc nominal), and current intensity can be an order of magnitude larger than ac railways. DC arcs in electrified transports have been characterized in the literature in terms of voltage-current relationship [1][3][4], typical waveforms and their spectra [5][6], and interaction with the traction line impedance and locomotive filter [2][7], exploiting them also for network impedance estimate [8].

In general, arcs are well known as a source of high-frequency noise potentially affecting the quality and availability of telecommunication and signaling systems [1][9]. The vast majority of studies and data are related to ac systems [10][11], in a high-speed modern railway perspective, although also dc systems have relevance, thinking of the many metros and rapid transits with integration of wireless signaling and services.

The presence of arcs at the pantograph-OCL interface (and similarly at the sliding shoe-third rail one) during traction is responsible for a first direct effect: the reduction of the available pantograph voltage V_p, since the arc voltage V_{arc} necessary for current conduction in plasma is in series with the line voltage V_l. Such reduction may in general cause a temporarily reduced train performance. Oppositely, arcs during braking increase the pantograph voltage due to the reverse flow of pantograph current [12], causing possible overvoltage issues.

Then, the arc conduction of the pantograph current I_p under a non-negligible voltage drop V_{arc} is responsible for a simple ohmic power loss, given by the product of the two quantities. For ac systems conduction losses were estimated by calculating the Lissajous diagram area between voltage and charge [13].

In addition, the electric arc as a broadband transient signal triggers the transient response of the traction network and train, causing the appearance of oscillations at the respective resonant frequencies, determined by the resonant filters at substation and onboard, and by the resonant modes of the line at higher frequency [2]. These components may disturb onboard metering and control [2], as well as signaling circuits connected to the track through the coupling of the return current [6][14].

A not so obvious consequence can be identified during regenerative braking: when arcing occurs, due to the direction of flow of I_p, the value of V_p is further increased and larger than the pre-arc line voltage. Dissipative braking by means of the braking chopper feeding onboard resistors can in this case start

due to momentarily excessive pantograph voltage, increasing conducted emissions and power losses.

This work models and analyses these cases including the explanation of the observed phenomena with the support of experimental results recorded over the Italian DC railway network and the Metro Madrid lines during the EMPIR 16ENG04 MyRailS project [12][15]. Section II discusses the electrical behavior of the arc, including the interaction with the traction line and the onboard filter. Section III then focuses on the power losses mechanisms for the identified phenomena, so as intrinsic arc dissipation, reduction of pantograph voltage and triggering of dissipative braking. Section IV reports and comments the experimental results.

II. Electric Arc and Interaction with Line and Vehicle

A. Electric arc

At the detachment of the pantograph from the catenary (or equivalently of the sliding shoe from the third rail) an electric arc may establish through one or more plasma columns that allow the flowing of the current through the air gap. The electric arc is maintained as long as the combination of air gap and available voltage is compatible with current conduction; in other words the electric arc requires a minimum voltage that depends on the pantograph current intensity I_p and gap width.

The typical V-I characteristic of dc arcs can be described as follows: i) at low current (e.g. tens of amperes) a constant arc power law can be assigned; ii) for increasing current above a specific threshold, the arc voltage reaches a plateau and does not depend then any longer on the current intensity. More complete dynamic models elaborated starting from Mayr's model can be found e.g. in [16], but the focus here is on power dissipation and so a quasi-static analysis is sufficient.

Of course V-I characteristics vary depending on electrode materials and for electrified transports also the relative movement of the electrodes plays an important role, for example increasing the effective arc length (the arc assumes an inclined position along the direction of movement). Various V-I curves for dc low-voltage arcs with static electrodes were collected by Paukert for current intensity ranging from 100 A to 100 kA [4].

The electric arc can thus be represented by the following Thevenin equivalent circuit: a resistor R_{arc}, variable with the intensity of the flowing current (getting smaller for increasing current), and a voltage source V_{arc} with values reaching a plateau for large I_p current intensity.

The arc resistance R_{arc} is in general negligible as shown in [17], Fig. 14, where values of 10 to 100 mΩ are reported. In case of various amounts of wearing after long use, the electric contact at the sliding surfaces worsens and the resistance increase by up to an order of magnitude [18]. The observed values during preliminary measurements [19] are of the same order (about 0.2 to 0.5 Ω).

B. Line resonances

Electric arcs as broadband transients can excite line resonances up to several tens of kHz (see Fig. 1), as shown in [2] using a parametric distributed-parameter model of the traction line and analyzing the components of the recorded electrical quantities. So, they are a relevant excitation source to probe the high-frequency portion of the line impedance and its resonance modes [8].

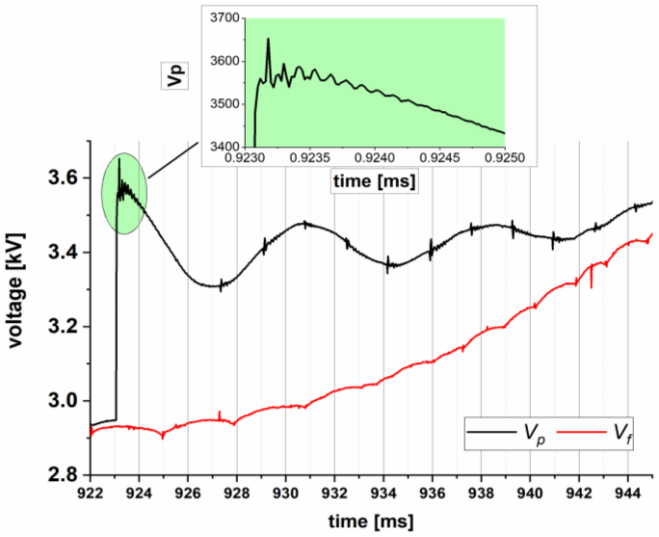

Fig. 1. Oscillations of the voltage V_p triggered by the re-establishment of the pantograph-to-line contact.

The transient terms of the resonant modes overlap in an initial burst following arc ignition (the portion of the arc waveform with the largest frequency content); the decay is also rapid since equivalent line resistance (sum of skin effect of catenary, additional losses in the rails [20] and distributed loads) is larger in that frequency range. As observed in [22], sec. III.C, line behavior at resonance and anti-resonance is purely resistive, increasing significantly the amplitude of harmonic active power terms. The phenomenon cannot be quantified, however, without a complex model of the entire line section and rolling stock items within it [22][23]. In [23] it was demonstrated that for dc vehicles the amount of harmonic power terms is limited, with amplitude much smaller than for ac railways and negligible.

The line resonance response remains thus relevant as a source of conducted disturbance appearing in the traction return current along the track and possibly coupling to audio-frequency track circuits, as analyzed in [24][25] for Italian high-speed lines.

C. Onboard filter transient response

The onboard LC filter is also excited by transients occurring at the pantograph interface, as well as by step loading during travel. Filter transient response occurs usually in the 12-25 Hz interval, determined mainly by the inductance and capacitance values of the onboard LC filter, although coupling with line and substation impedance (the latter featuring a similar LC output filter) can slightly modify the response. The large-value series inductor during the transient response behaves as a high impedance current source imposing an oscillating current in the I_p waveform and flowing along the line section. This behavior was analyzed in [2], identifying the conditions for the flow of current back to the substation through the rectifier diodes when positively biased by other trains pulling traction current within the same supply section. The absence of this condition prevents the flow through the otherwise reverse-biased rectifier diodes and causes anticipated arc quenching; at the successive I_p oscillation the arc can re-ignite if the pantograph detachment condition holds. The combined effect of the non-linear conductance of the diodes and the excitation of the first line resonance slightly above 100 Hz can be seen in Fig. 2.

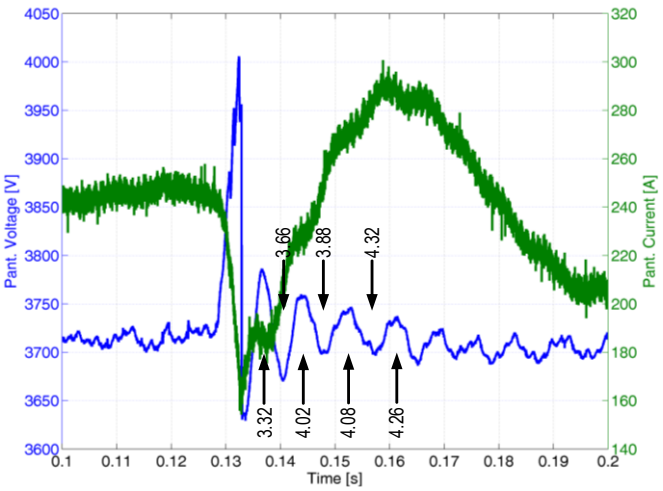

Fig. 2. Oscillations of voltage V_p at the first line resonance (slightly above 100 Hz) and difference in positive and negative half-cycles duration caused by the non-linear conduction of substation diodes (reproduced from [2]).

III. Modeling Power Losses

A. Electric arc dissipated power

The arc resistance is extremely small and does not contribute significantly to circuit damping; the arc conduction voltage instead appears suddenly at arc ignition and represents the main electric phenomenon related to the arc event. Power dissipation within the electric arc, as a non-linear resistance element, is thus calculated straightforwardly as $P_{arc}=V_{arc}I_p$.

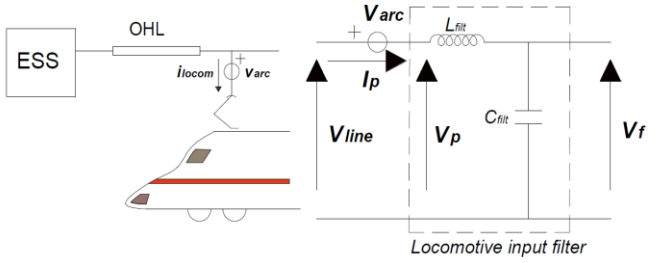

Fig. 3. Simplified scheme of the electrical quantities during an electric arc occurring at pantograph.

B. Reduction of useful voltage

As sketched in Fig. 3, the arc voltage is in series to the line voltage with respect to the pantograph, so that $V_l - V_{arc} = V_p$, having noted the arc voltage with load convention, so towards the line with a positive incoming I_p current. This reveals two opposite behaviors, during traction with a reduction of available voltage (being $V_{arc}>0$) and during braking with an increase of V_p beyond line voltage (being $V_{arc}<0$), possibly triggering protection by dissipative braking, as discussed below in sec. III.C.

Considering an arc event occurring during a traction phase, V_p rapidly falls down while the voltage downstream the filter inductor is kept constant by the large filter capacitance. This imbalance across the filter inductor triggers a current oscillation at the filter natural frequency with a negative derivative. Therefore, at the occurrence of an arc event during traction, V_p and I_p decrease with different time behavior, and the power fed to the traction unit dramatically decreases for a short time interval. If the arc occurs in correspondence of a small absorbed current I_p, with the superposed oscillation negative values might be reached; however, when the current reaches zero the arc quenching occurs. In this case, with the extinction of the arc at zero current the locomotive is completely disconnected from the catenary and the energy stored in the filter capacitor feeds the circuits downstream; as long as the capacitor discharges the voltage across it V_f gets smaller. Because of the pantograph detachment and the zero flow of current in the filter inductor, the pantograph voltage V_p tracks V_f. This is demonstrated by the change of ripple in V_p: before quenching V_p is characterized by the typical 100, 300 and 600 Hz ripple caused by the substation [2][6]; with the arc quenching the V_p ripple is equal to the V_f ripple that is caused by the traction inverters.

C. Triggering dissipative braking

As previously mentioned, during regenerative braking the current I_p is applied into the network and the arc voltage sign reverses and increases the pantograph voltage V_p beyond the line voltage V_l.

It is customary to implement a safety mechanism, so that the local line voltage (sensed by measuring V_f) cannot go beyond a given threshold (usually corresponding to the maximum permanent voltage of the EN 50163). During detachment and triggering of electric arc the V_p quantity does not follow closely the line voltage V_l any longer, and the detection of the threshold voltage is anticipated. A phase of dissipative braking by means of the braking chopper starts to keep the supposed line voltage V_p stable, thus causing increased power losses and conducted disturbance.

IV. Experimental Assessment

A. Arc event during a traction phase

Two arc events are analyzed in terms of dissipated energy. The first event is shown in Fig. 4 and a zoom around the arc event in Fig. 5. The event is characterized by a voltage reduction of about 300 V and the absorbed current, because of the superposed filter oscillation, goes from 200 A to 0 A (arc quenching). The arc duration is about 14.9 ms while the quenching phase lasts for about 70 ms. At the end of the quenching the contact between the pantograph and the OCL is re-established with a very fast increase of V_p, reaching again approximately the same amplitude before the arc event (about 3.6 kV). This voltage step, characterized by a slew rate of about 14.8 V/μs, triggers the filter oscillation at about 15 Hz.

The average power dissipated by the arc, computed over its duration (14.9 ms) is 6.2 kW, corresponding to an energy of 93 J. For what concerns the active power associated with the oscillation phase, Table I summarizes the results for each of the first three oscillation periods: the active power terms are calculated by considering V_p and I_p and separating them into a dc and an ac component, assigning to the arc phenomenon those terms that include at least one ac component. The table also provides the dc power that the locomotive should have absorbed if the arc event had not occurred.

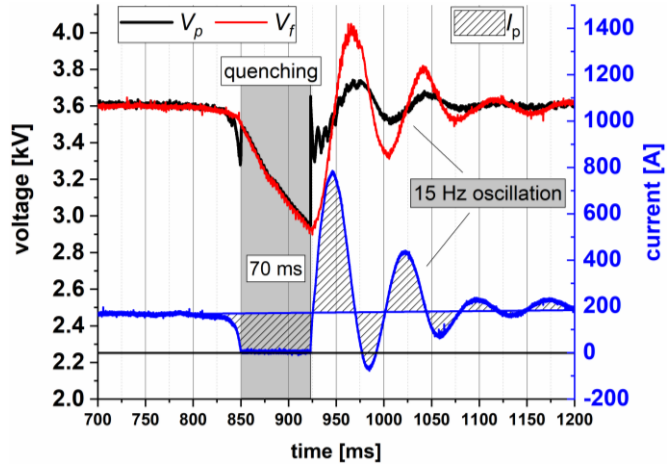

Fig. 4. Arc event during a traction phase and consequent quenching.

TABLE I. ACTIVE POWER RELATED TO THE 15 HZ OSCILLATION [KW]

Calc. power term	period 1	period 2	period 3
full V_p × full I_p	1167	851	694
V_p (ac comp.) × full I_p	20.3	3.09	2.6
full V_p × I_p (ac comp.)	495.6	177.5	197.4
V_p (dc comp.) × I_p (dc comp.)	673.2	673.2	673.2

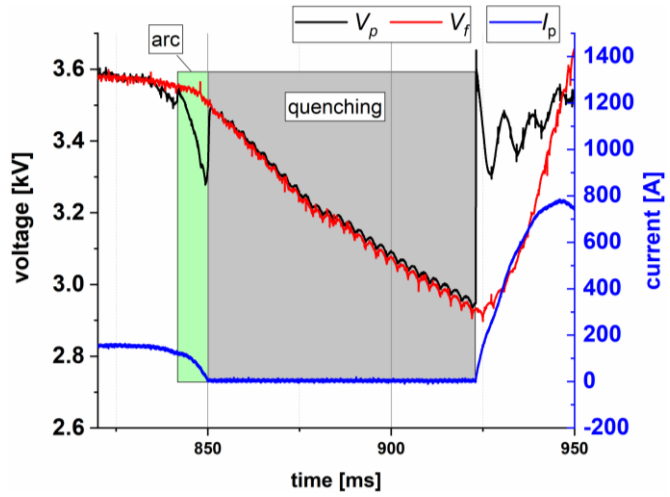

Fig. 5. Zoom of the arc event shown in Fig. 4.

B. Arc Event during a regenerative braking phase

Fig. 5 shows the electric arc event during a regenerative braking where the energy is subdivided into a part of recovered energy used to supply other loads along the line and into a remaining part of energy dissipated by the braking rheostats. As previously mentioned, during the braking phase the arc voltage V_{arc} is negative; therefore, the voltage measured at the pantograph, V_p, will be larger than the line voltage V_l.

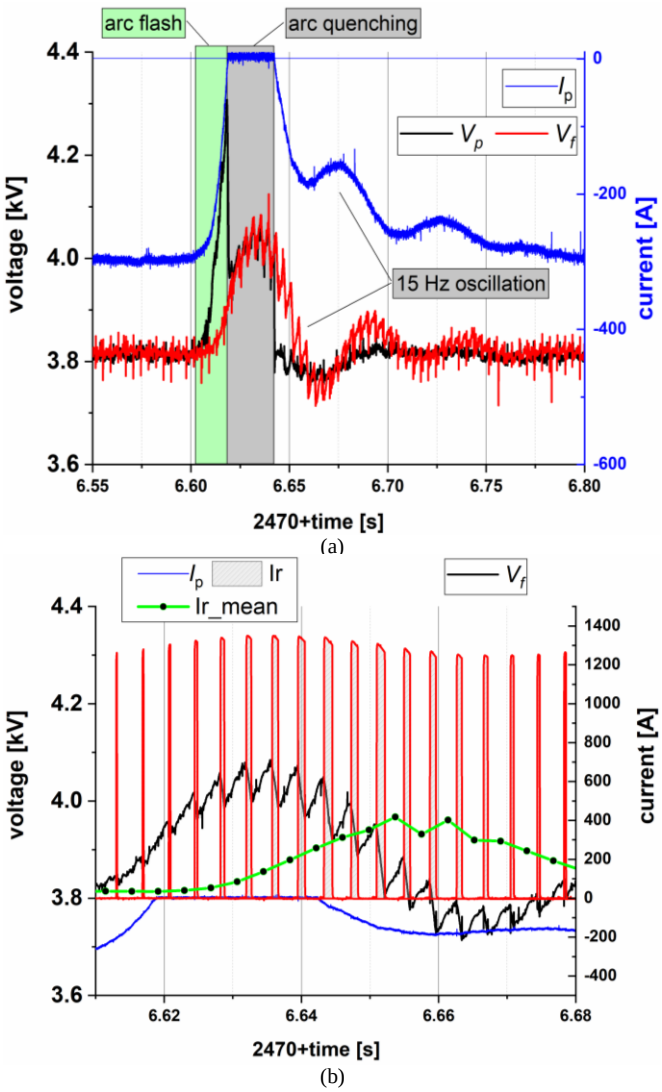

Fig. 6. Arc event during regenerative braking: (a) details of arc flash and arc quenching with damped 15 Hz oscillation; (b) waveform of the dissipative braking chopper control superposed to voltage and current waveforms.

In Fig. 6(a) the arc flashing phase, highlighted in green, is characterized by a voltage impulse of about 450 V rising in about 10 ms. In the same time span, the current decreases to zero, arriving at the arc quenching phenomenon, highlighted in grey. For about 25 ms, as for the arc during the traction phase examined in sec. III.A, the current is zero and the voltage upstream (V_p) and downstream (V_f) of the filter are equal. As can be seen in Fig. 6(b), in this interval not only the braking type changes from mixed to purely dissipative, but the train control system increases the duty cycle of the chopped rheostatic current to counteract the increase of V_p. In the phase following arc quenching, the pantograph voltage quickly returns to the line voltage, triggering the low frequency oscillation of the filter. The mean power dissipated by the arc is 25 kW. As can be seen in Fig. 7 the arc event with the consequent voltage swell also increases the power dissipated by the rheostat reaching a maximum value of 1.65 MW. The mean value of the additional power dissipated by the rheostat because of arc occurrence is 152 kW.

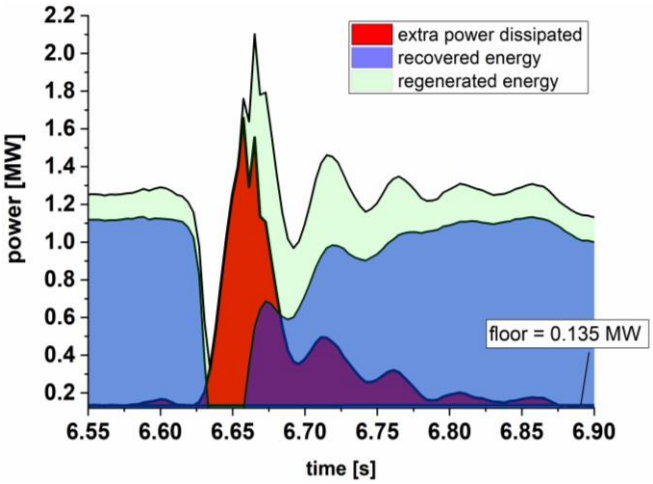

Fig. 7. Time behavior of the extra-power dissipated by the braking rheostat (red), the recovered power sent back to the catenary (dark blue) and the total regenerated power (light blue).

V. Conclusions

This work has considered the occurrence of pantograph arcs of a dc railway system during traction and braking phases. In both cases the voltage waveforms and the physical phenomena have been analyzed, to understand the dynamics of the arc discharge, its evolution and possible quenching when the pantograph current reaches zero.

In particular, the dissipated power terms associated to the arc itself and to the electric phenomena (oscillation of the onboard filter) and events (activation of the dissipative braking chopper) have been evaluated, showing that the peak power levels are notable. Despite the short duration of the arc, also the energy values are not negligible, especially considering the rate of repetition of electric arc in dc traction systems.

Acknowledgement

The presented activity was performed within the 16ENG04 MyRailS Project of the European Metrology Programme for Innovation and Research (EMPIR), jointly funded by the European Union's Horizon 2020 research and innovation programme and the EMPIR participating states. This work was also supported by the Swiss State Secretariat for Education, Research and Innovation (SERI) under contract no. 17.00127. The opinions expressed and arguments employed herein do not necessarily reflect the official views of the Swiss Government.

References

[1] G. Crotti *et al.*, "Pantograph-to-OHL arc: Conducted effects in DC railway supply system," *IEEE Trans. Instrum. Meas.*, Vol. 68, No. 10, pp. 3861-3870, 2019.

[2] A. Mariscotti and D. Giordano, "Experimental Characterization of Pantograph Arcs and Transient Conducted Phenomena in DC Railways," *Acta Imeko*, Vol. 9, No. 2, pp. 10-17, June 2020.

[3] R. F. Ammerman and P. K. Sen, "Modeling High-Current Electrical Arcs: A Volt-Ampere Characteristic Perspective for AC and DC Systems," 39th North Am. Pow. Symp., Las Cruces, New Mexico, USA, 2007, pp. 58-62.

[4] J. Paukert, "The Arc Voltage and the Resistance of LV Fault Arcs," Proc. 7th Intern. Conf. Switching Arc Phenom., Lodz; Poland, 1993, pp 49-51.

[5] S. Midya *et al.*, "Pantograph Arcing in Electrified Railways—Mechanism and Influence of Various Parameters—Part I: With DC Traction Power Supply," *IEEE Trans. Pow. Del.*, Vol. 24, No. 4, Oct. 2009, pp. 1931-1939.

[6] A. Mariscotti, "Characterization of power quality transient phenomena of DC railway traction supply," *Acta Imeko*, Vol. 1, No. 1, pp. 26-35, 2012.

[7] A. Mariscotti and D. Giordano, "Electrical Characteristics of Pantograph Arcs in DC Railways: Infrastructure Influence," 23rd IMEKO TC4 Intern. Symp., Xi'an, China, Sept. 17-20, 2017.

[8] A. Mariscotti *et al.*, "Filter Transients onboard DC Rolling Stock and Exploitation for the Estimate of the Line Impedance," Proc. of IEEE Intern. Instrum. Meas. Tech. Conf., Dubrovnik, Croatia, May 25-28, 2020.

[9] A. Mariscotti *et al.*, "Time and frequency characterization of radiated disturbance in telecommunication bands due to pantograph arcing," *Measurement*, Vol. 46, pp. 4342-4352, 2013.

[10] G. Gao *et al.*, "A pantograph arcing model for electrified railways with different speeds," *Proc Inst. Mech Eng Part F: J Rail and Rapid Transit*, Vol. 32, No. 6, 2018, pp. 1731-1740.

[11] G. Wu *et al.*, "Characteristics of the Sliding Electric Contact of Pantograph/Contact Wire Systems in Electric Railways," *Energies*, Vol. 11, No. 17, 2018.

[12] D. Signorino *et al.*, "Dataset of measured and commented pantograph electric arcs in DC railways," *Data in Brief*, Vol. 31, 105978, July 2020.

[13] W. Wang *et al.*, "Experimental Study of Electrical Characteristics on Pantograph Arcing," 1st Intern. Conf. on Electr. Pow. Equip. – Switching Techn., Xi'an, China, 2011.

[14] S. Yang, J. Tian, H. Xu, Y. Cui, L. Chen, "Analysis on harmonic current and its impact on track circuit in high speed railway," Proc. of IEEE Intern. Conf. Intell. Rail Transp. (ICIRT), Birmingham, UK, Aug. 23-25, 2016.

[15] MyRailS, Metrology for Smart Energy Management in Electric Railway Systems, https://myrails.it

[16] A. Sawicki, "Arc models for simulating processes in circuits with a SF6 circuit breaker," *Arch. of Electr. Eng.*, Vol. 68, no. 1, pp. 147-159, 2019.

[17] G. Bucca and A. Collina, "A procedure for the wear prediction of collector strip and contact wire in pantograph–catenary system," *Wear*, Vol. 266, pp. 46-59, 2009.

[18] V. V. Terzija and H. J. Koglin, "On the Modeling of Long Arc in Still Air and Arc Resistance Calculation," *IEEE Trans. Pow. Del.*, Vol. 19, No. 3, pp. 1012-1017, July 2004.

[19] G. Crotti *et al.*, "Pantograph-to-OHL Arc: Conducted Effects in DC Railway Supply System," Proc. of 9th IEEE Intern. Workshop on Applied Meas. for Pow. Sys. (AMPS), Sept. 26-28, 2018, Bologna, Italy.

[20] F. Filippone, A. Mariscotti, P. Pozzobon, "The Internal Impedance of Traction Rails for DC Railways in the 1-100 kHz Frequency Range", *IEEE Trans. Instrum. Meas.*, Vol. 55, No. 5, pp. 1616-1619, Oct. 2006.

[21] A. Mariscotti, "Impact of Rail Impedance Intrinsic Variability on Railway System Operation, EMC and Safety," *Int. J. Electr. Comput. Eng. (IJECE)*, Vol. 11, No. 1, Feb. 2021.

[22] A. Mariscotti, "Impact of Harmonic Power Terms on the Energy Measurement in AC Railways," *IEEE Trans. Instrum. Meas.*, Vol. 69, No. 9, pp. 6731-6738, Sept. 2020.

[23] A. Mariscotti, "Characterization of Active Power Flow at Harmonics for AC and DC Railway Vehicles," IEEE Veh. Pow. and Prop. Conf., Oct. 14-17, 2019, Hanoi, Vietnam.

[24] S. Ciurlo and A. Mariscotti, "Track compensation with Audiofrequency Track Circuits", Proc. Intern. Conf. on Electr. Sys. for Aircraft, Railway and Ship Prop. (ESARS), Bologna, Italy, Oct. 21-23, 2010.

[25] A. Mariscotti, M. Ruscelli, M. Vanti, "Modeling of Audiofrequency Track Circuits for validation, tuning and conducted interference prediction", *IEEE Trans. Intell. Transp. Sys.*, Vol. 11, no. 1, pp. 52-60, March 2010.

[26] A. Mariscotti, "Experimental characterization of active and nonactive harmonic power flow of AC rolling stock and interaction with the supply network," *IET Electr. Sys. Transp.*, 2020, in press.